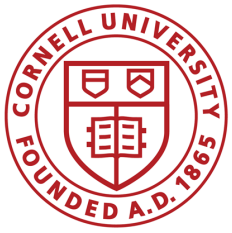

Evaluating Steady State Volcanism
in Iceland, La Réunion, Hawaii and Western Galápagos:
connections with volcanic hazard and future perspectives
Data Analysis and Prediction

Beatriz Asfora, Federico Galetto - Version #8
July 28, 2025

1 Overview

Volcanoes exhibiting steady state activity erupt magma at approximately constant rates, but the extent to which this behavior occurs globally is still uncertain. This study examines four frequently erupting oceanic hot spots – Iceland, La R'eunion, Hawaii, and the Western Galápagos – to assess the reliability of steady state volcanism in forecasting volcanic hazards. The results indicate that eruptive rates commonly fluctuate, with phases of reduced activity offset by later increases (and vice versa), allowing for **reasonably accurate volume predictions**, though not eruption timing.

2 Historical Data

2.1 Piton de la Fournaise

Located on the French island of Réunion in the western Indian Ocean, Piton de la Fournaise has had more than 150 eruptions since the 17th century[1]. We have compiled its most recent eruptive history into two periods, with *eruption end dates* as follows:

- Period I: 1936-08-01 to 1998-03-11, Fig. 1
  73 eruptions, rate of eruption $Q_{\mathrm{I}} = 0.0107\ \mathrm{km}^3/\mathrm{yr}$
- Period II: 1997-07-19 to 2018-07-13 Fig. 2
  46 eruptions, rate $Q_{\mathrm{II}} = 0.0228\ \mathrm{km}^3/\mathrm{yr}$

Fig.**(1)** to Fig.**(3)** show the erupted volume per event and the time interval between successive eruptions[2].

[1] Source: Smithsonian Institution - Global Volcanism Program.
[2] NOTE: Full resolution images can be found in the figures folder.

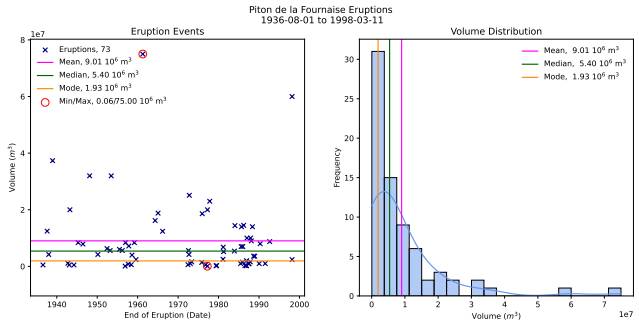

(a) Eruption volume (LEFT) and distribution (RIGHT)

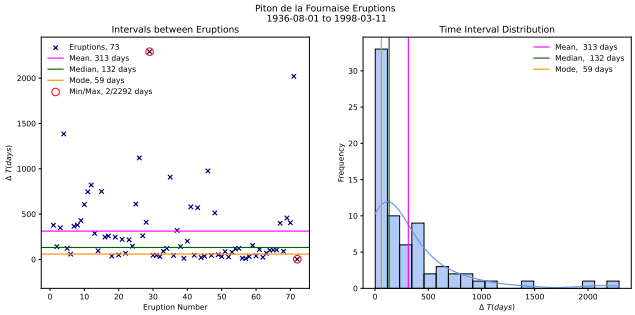

(b) Time interval between eruptions.

Figure 1: Piton de la Fournaise, Period I (1936-08-01 to 1998-03-11).

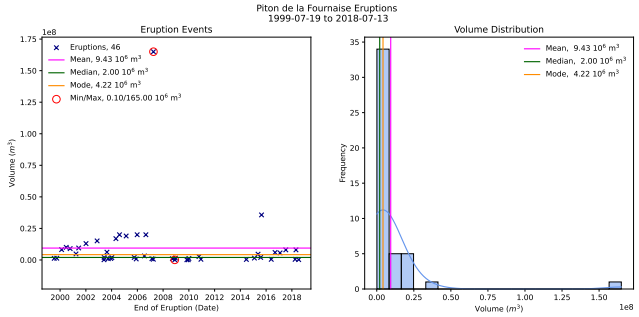

(a) Eruption volume (LEFT) and distribution (RIGHT)

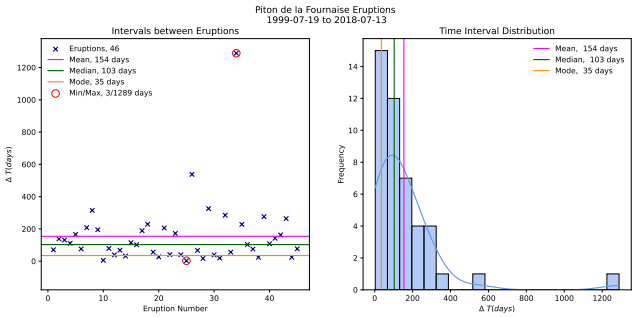

(b) Time interval between eruptions.

Figure 2: Piton de la Fournaise, Period II (1997-07-19 to 2018-07-13).

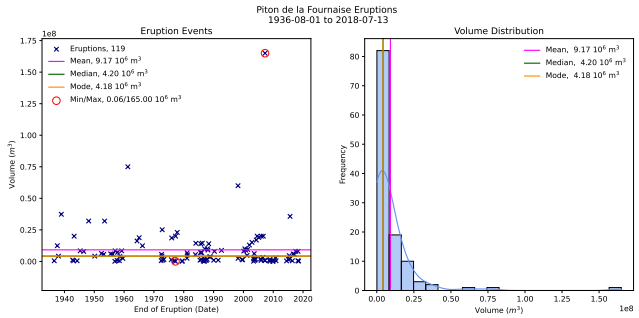

(a) Eruption volume (LEFT) and distribution (RIGHT)

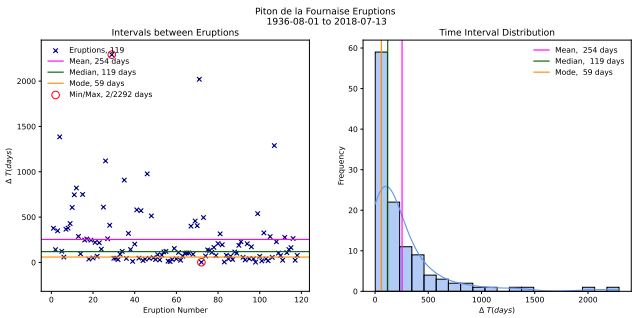

(b) Time interval between eruptions.

Figure 3: Piton de la Fournaise, both Periods (1936-08-01 to 2018-07-13).

When analyzing these variables, separately for the two time periods, as well as for the combined dataset, their distributions consistently display *right-skew normal* characteristics [1]. For example, the eruption volume for Period I presents sparse extreme events (high-end outliers shown in Fig.**(1a)**), increasing the mean of the dataset. Note in Fig. 1a that the mode is smaller than the median, which is in turn smaller than the mean (mode < median < mean), contrasting with the symmetric normal distribution (mean = median = mode) often assumed in the analysis of natural phenomena. Similar behavior is observed for the eruption volume data for all periods analyzed. For the time intervals between consecutive eruptions' end dates, the right-skewedness is even more pronounced, complicating efforts to predict the timing of the next eruption.

2.2 Iceland

Recent eruptive history with eruption *end* dates as follows:

- Period I: 1961-12-05 to 2024-11-21, Fig.**(4)** – 28 eruptions, rate $Q_{\mathrm{I}} = 0.1110$ km^3/yr

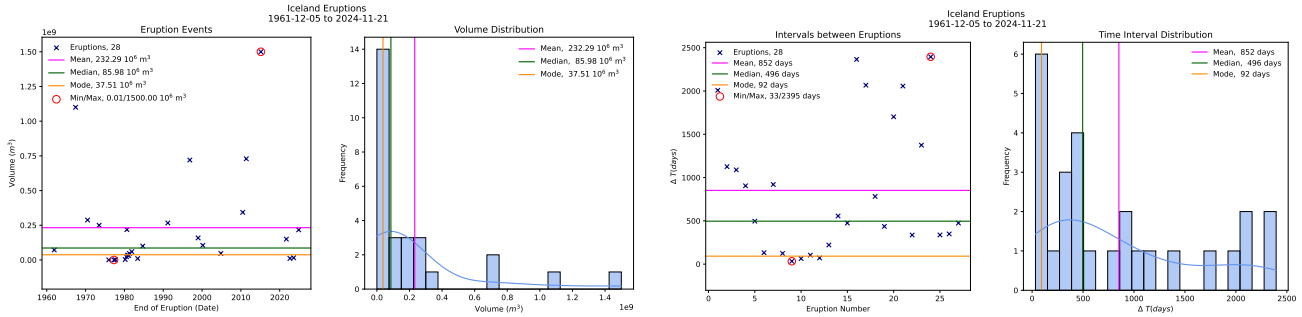

(a) Eruption volume (LEFT) and distribution (RIGHT) (b) Time interval between eruptions.

Figure 4: Iceland, Period I (1961-12-05 to 2024-11-21).

2.3 Hawaii

Recent eruptive history with eruption *end* dates as follows:

- Period I: 1923-08-26 to 1984-04-15, Fig. Fig.**(5)** 53 eruptions, rate of eruption $Q_{\mathrm{I}} = 0.0405$ km^3/yr
- Period II: 1986-06-26 to 2018-08-05, Fig.**(6)** 10 eruptions, rate $Q_{\mathrm{II}} = 0.2149$ km^3/yr

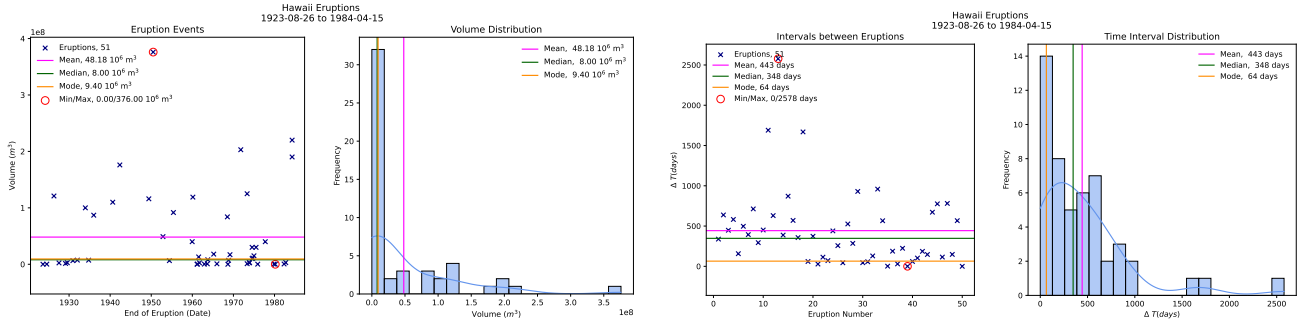

(a) Eruption volume (LEFT) and distribution (RIGHT) (b) Time interval between eruptions.

Figure 5: Hawaii, Period I (1923-08-26 to 1984-04-15).

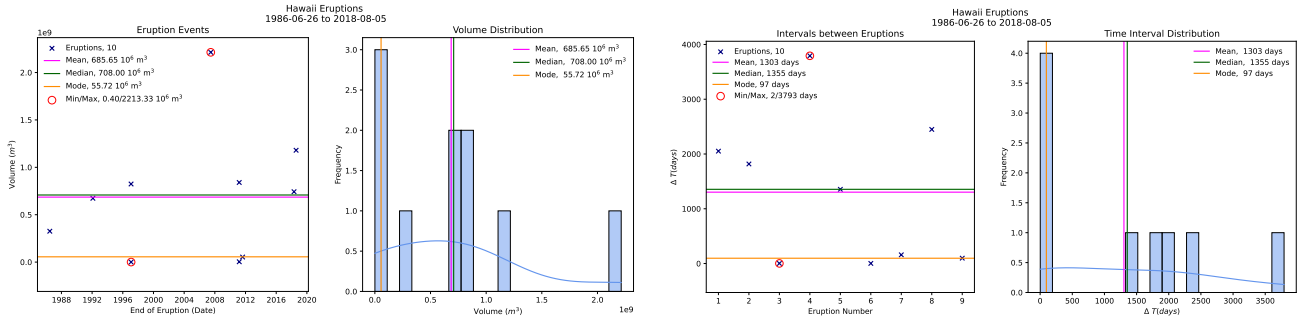

(a) Eruption volume (LEFT) and distribution (RIGHT) (b) Time interval between eruptions.

Figure 6: Hawaii, Period II (1986-06-26 to 2018-08-05).

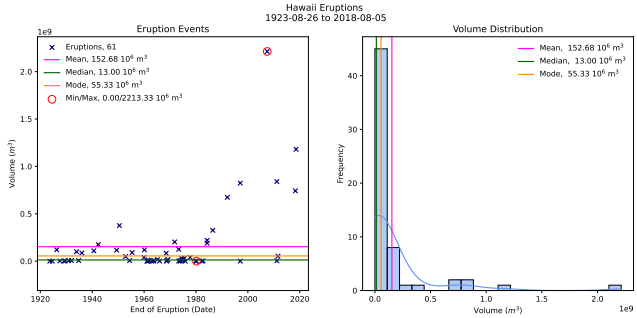

(a) Eruption volume (LEFT) and distribution (RIGHT)

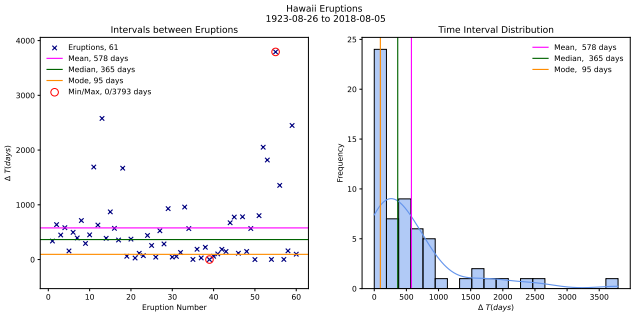

(b) Time interval between eruptions.

Figure 7: Hawaii, both Periods (1923-08-26 to 2018-08-05).

2.4 Western Galápagos

Recent eruptive history with eruption *end* dates as follows:

- Period I: 1988-09-16 to 2024-05-08, Fig. Fig.**(8)** – 15 eruptions, rate $Q_{\mathrm{I}} = 0.0240$ km^3/yr

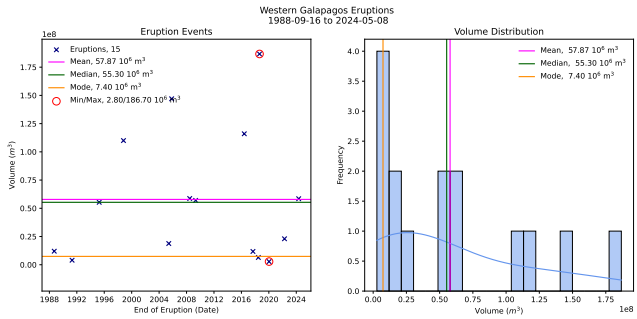

(a) Eruption volume (LEFT) and distribution (RIGHT)

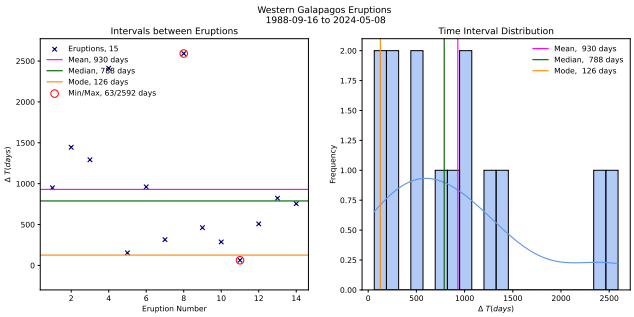

(b) Time interval between eruptions.

Figure 8: Western Galápagos, Period I (1988-09-16 to 2024-05-08).

3 System Modeling

We aim to estimate the volume of future eruptions – specifically, the next eruption – given historical records of individual eruption volumes (*evol*), cumulative volume following each eruption (*cvol*), and the time interval between eruptions (Δt).

3.1 Process Equation

Consider the linear state equation for our steady-state volcano system:

$$cvol(t_2) = Q \times (t_2 - t_1) + cvol(t_2), \tag{1}$$

where $cvol(t_2)$ is the state we want to predict, i.e., the resulting cumulative volume after the next eruption; $cvol(t_1)$ is the cumulative volume at a given time t_1, and Q is the steady-state eruptive rate.

Equation (1) is directly derived from the calculation of the eruptive rate Q:

$$Q = \frac{cvol(t_2) - cvol(t_1)}{\Delta t}, \tag{2}$$

where $\Delta t = t_2 - t_1$ is the time interval between the end of eruptions (in days). Although the eruptive rate is often converted to km^3/yr for better visualization, our calculations and plots might employ the units m^3/days.

We present three possible methods for estimating the expected cumulative volume ($cvol$) after the next eruption. The latest volume $cvol(t_1)$ and end time of latest eruption t_1 are always considered known.

[In the paper, we should name these methods as you prefer, so we can refer to them consistently.]

3.2 Method 1: Q-Line Fit

The eruptive rate for each significant period is computed as shown in Eq. (2), with t_1, t_2 equal to the first and last eruption of the period, respectively. The periods and respective rates for Piton de la Fournaise are listed on Sec. 2.1. Potential application: This fitted line can then be used for linear extrapolation to estimate the cumulative volume at a future time, and thereby predict the volume of the next eruption.

Fig.**(9)** (top) illustrates the q-line fit applied to the cumulative volume for each period studied. The corresponding error distribution is shown in Figure Fig.**(9)** (bottom), with error mean and standard deviation -0.0021 ± 0.0411 km^3. More error characteristics are shown in Table 1. The other three volcanoes are shown in Fig.**(10)**, Fig.**(11)**, and Fig.**(12)**.

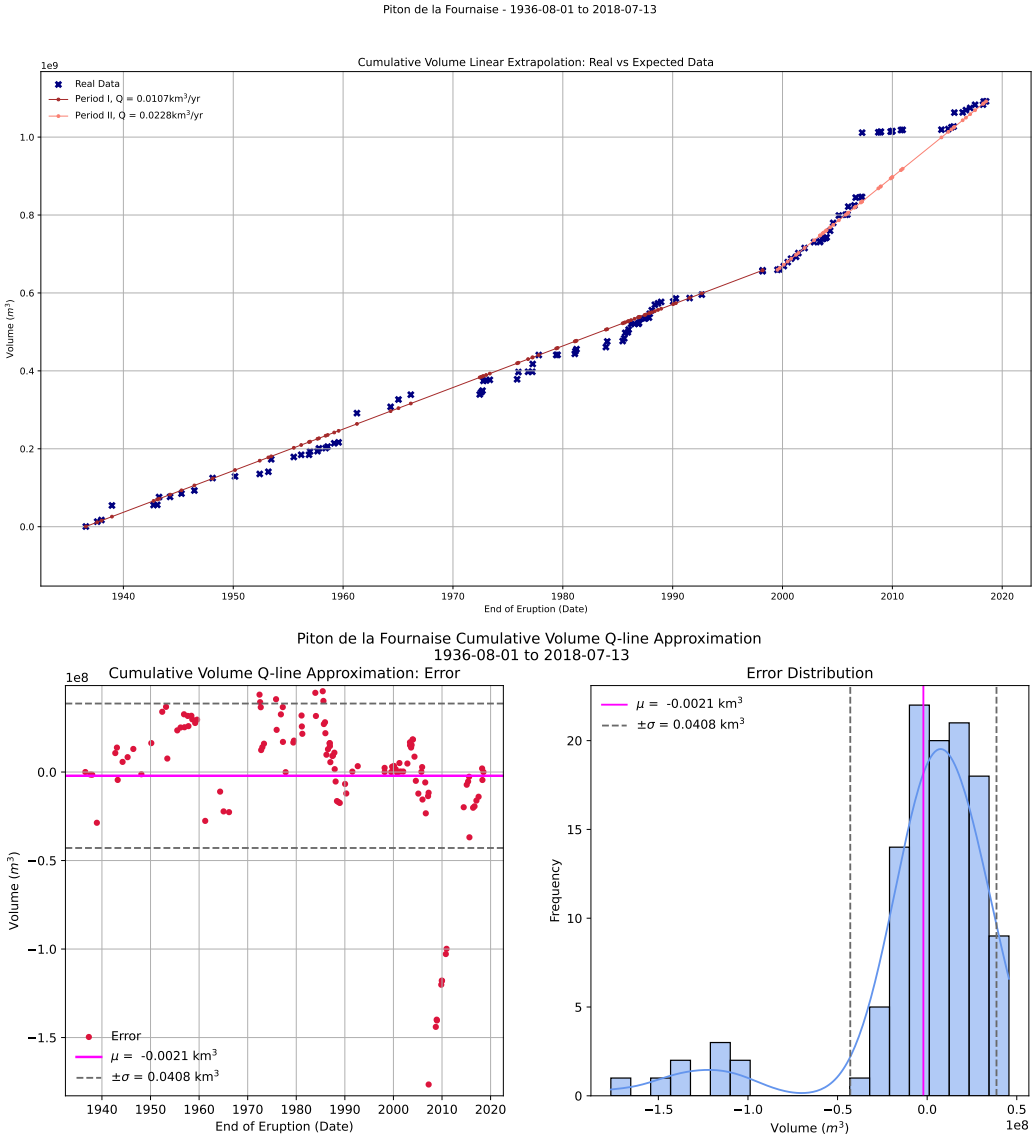

Figure 9: Piton, cumulative eruption volume: real data vs Q-line fit. TOP: Expected vs real data; BOTTOM LEFT: Error; BOTTOM RIGHT: Error distribution.

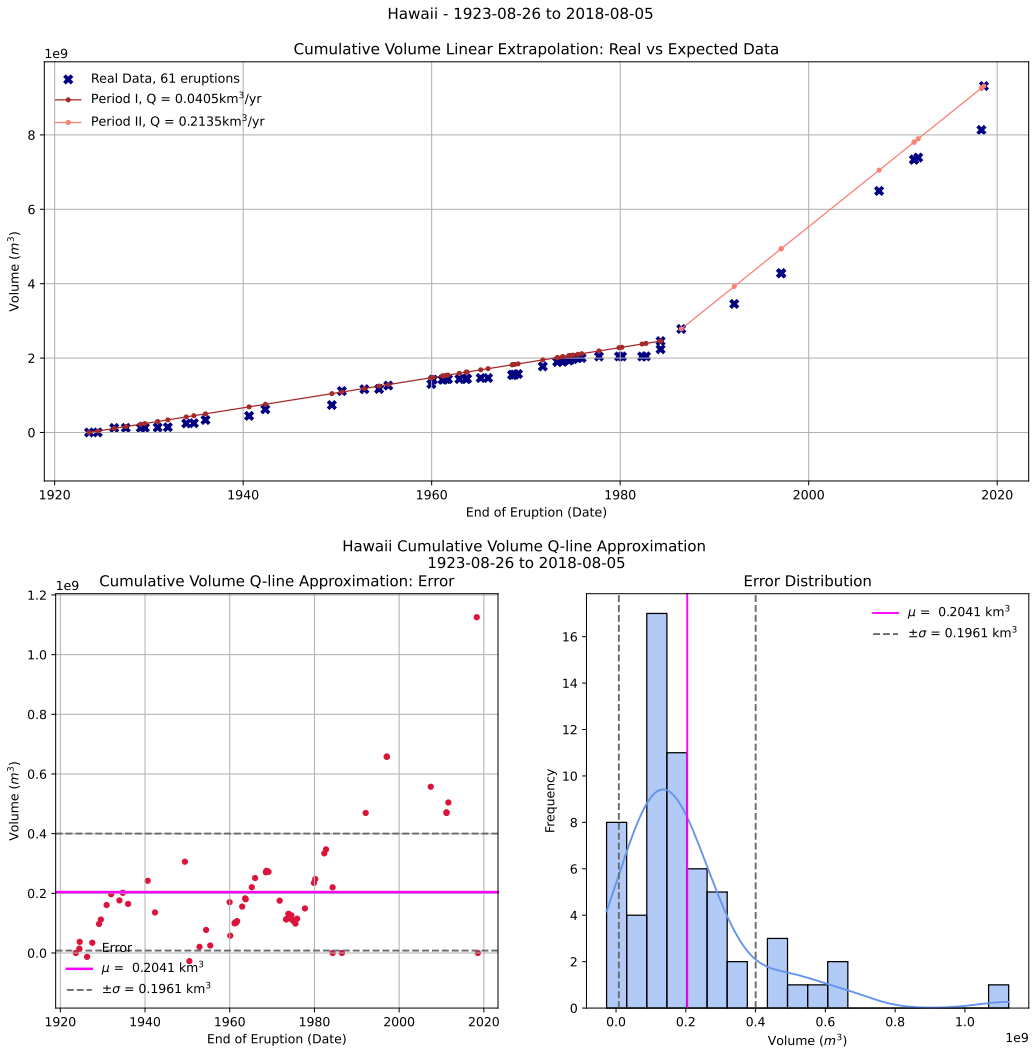

Figure 10: Hawaii, cumulative eruption volume: real data vs Q-line fit. TOP: Expected vs real data; BOTTOM LEFT: Error; BOTTOM RIGHT: Error distribution.

3.3 Method 2: Deterministic Time Interval

3.3.1 Validation

Consider our state equation (Eq. 1), where $cvol(t_1)$ is the cumulative volume after the last eruption that ended by t_1, and Q is the known eruptive rate for each period considered, respectively $Q_{\mathrm{I}} = 0.0107$ and $Q_{\mathrm{II}} = 0.0228$ km^3/yr. Fig. Fig.**(13)** (top) shows the results using these parameters, along with the actual time interval between eruptions (Δt), in the state equation. The corresponding error distribution is shown in Figure Fig.**(13)** (bottom), with error mean and standard deviation 0.0003 ± 0.0221 km^3. More error characteristics are shown in Table 1.

Figure Fig.**(13)** demonstrates that Eq. (1) provides a reasonable approximation for the expected cumulative volume following the last known eruption. The resulting error exhibits an approximately zero-mean Gaussian distribution (see Fig. Fig.**(13)**, bottom), as evidenced by its bell-shaped curve and the alignment of mean, mode, and median. This suggests that the estimation is unbiased and that the residual variability is largely attributable to random noise. Overall, Eq. (1) seems to effectively capture the underlying process dynamics in a simple manner.

The other three volcanoes are shown in Fig.**(14)**, Fig.**(15)**, and Fig.**(16)**.

3.3.2 Potential Application

While it is generally accepted within the research community that the exact timing of the next eruption at a steady-state volcano cannot be predicted, this equation can still be used to explore a range of plausible eruption intervals and to map out potential future scenarios. [Let me know if/which range you want me to plot - I have the code pretty much setup but did not know the specifics]

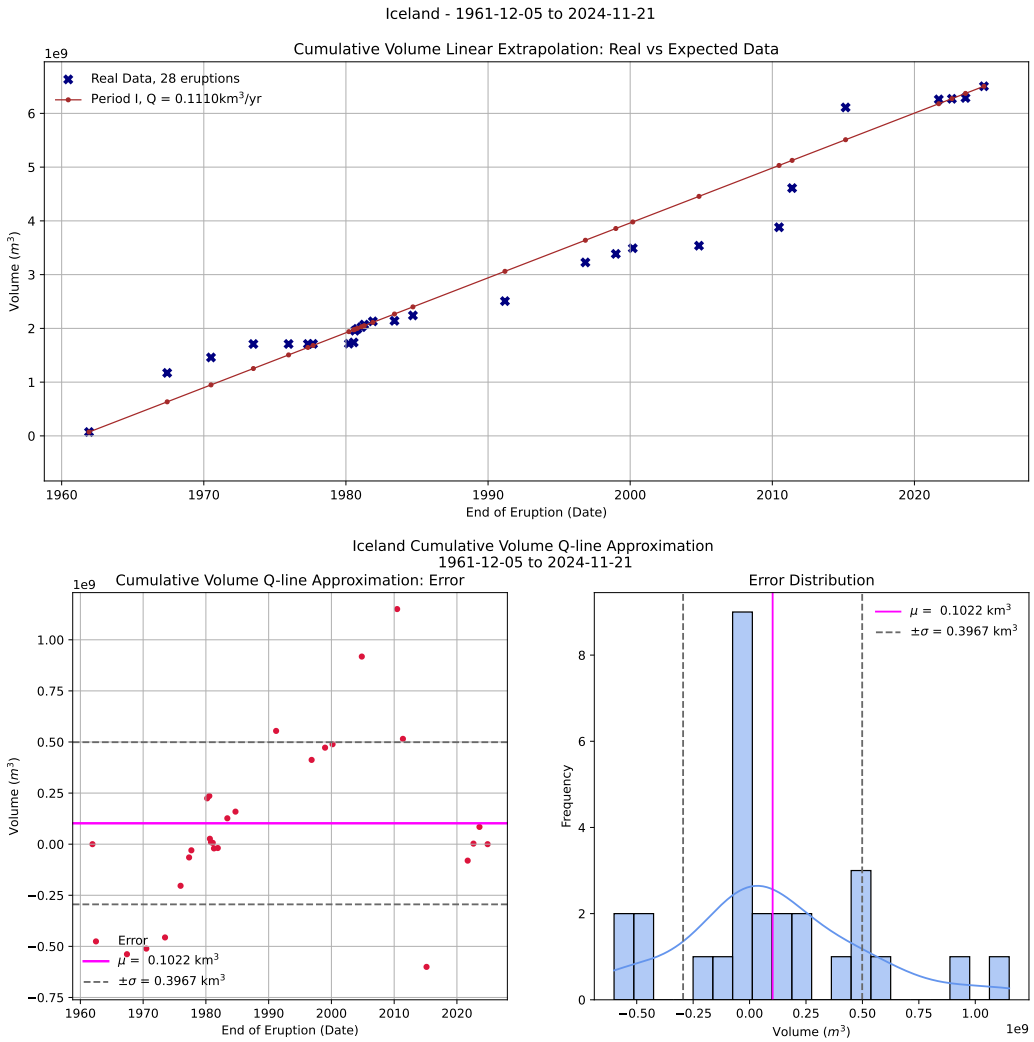

Figure 11: Iceland, cumulative eruption volume: real data vs Q-line fit. TOP: Expected vs real data; BOTTOM LEFT: Error; BOTTOM RIGHT: Error distribution.

4 Error Analysis

4.1 Metrics

Consider the notation

- x: real value (measurement data from previous volcano eruptions)
- $\hat{x}$: expected value (estimated using one of our described methods)

Error values are computed as follows:

- **Error** (residual): difference between expected and real value, shown in Fig.**(9)** - Fig.**(16)** - bottom-left $\rightarrow \; e = \hat{x} - x$
- **Error mean**: average of the residuals, for n eruptions $\rightarrow \; \mu_e = \frac{1}{n}\sum_{i=1}^{n} e_i$
- **Error standard deviation**: how much the error varies around its average value, indicates the consistency of the estimations (lower is better) $\rightarrow \sigma_e = \sqrt{\frac{1}{n}\sum_{i=1}^{n}(e_i - \mu_e)^2}$
- **Mean Squared Error (MSE)**: average of the squares of the errors, captures both how spread out and how biased the estimates are $\rightarrow \text{MSE} = \frac{1}{n}\sum_{i=1}^{n}(\hat{x} - x)^2$
- **Root Mean Squared Error (RMSE)**: square root of the MSE, converts it back to the original units for easier interpretation $\rightarrow \; \text{RMSE} = \sqrt{\frac{1}{n}\sum_{i=1}^{n}(\hat{x} - x)^2}$

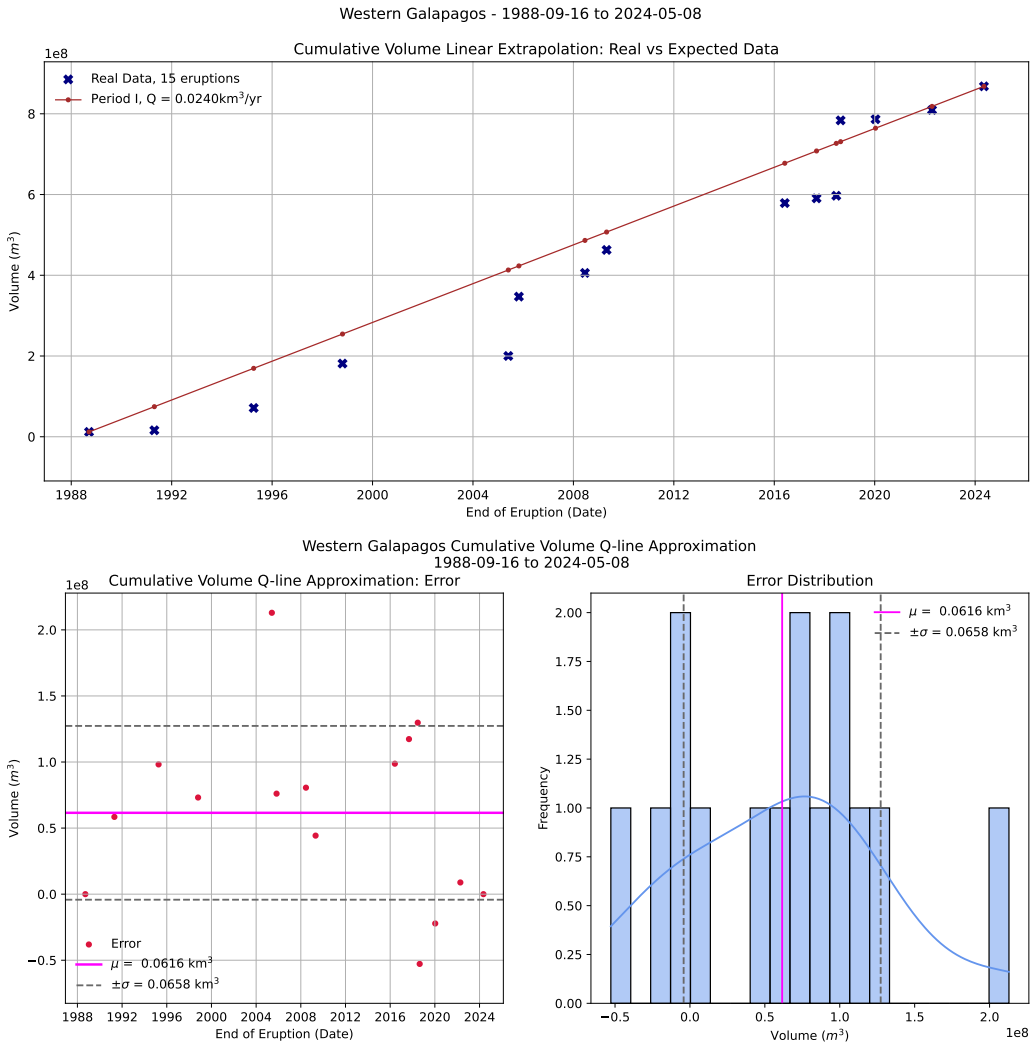

Figure 12: Iceland, cumulative eruption volume: real data vs Q-line fit. TOP: Expected vs real data; BOTTOM LEFT: Error; BOTTOM RIGHT: Error distribution.

- **Absolute error**: distance between expected and real value, for 1 dimensional error values → $|e| = \sqrt{(\hat{x} - x)^2}$
- **Max absolute error** (MAX): largest absolute error, worst-case scenario → $\max(|e_1|, |e_2|, .., |e_n|)$ for n eruptions.
- **Percetage error** (%): how large the error is relative to the real value, as a percentage → $\left|\frac{\hat{x} - x}{x}\right| \times 100$

4.2 Comparison between Methods

Table 1 shows the error characteristics between theoretical and historical data when using linear regression (method I) and state equation with known time interval (method II). Note that both methods are unbiased, with standard deviation of residuals being equal to RMSE.

Although the mean and maximum error values for Methods I and II are relatively close, the error dispersion of Method II is roughly half of Method I. This indicates that Method II produces more consistently accurate estimates, with reduced deviation from true values and less sensitivity to random fluctuations.

	Mean ± Std Dev $\mu_e \pm \sigma_e (km^3)$	MAX $\max \lvert e \rvert\ (km^3)$	RMSE (km^3)
Method **I**	-0.0021 ± 0.0411	0.1765	0.041202
Method **II**	0.0003 ± 0.0221	0.1648	0.022094

Table 1: Error characteristics for Method I (linear regression) and II (state equation). |.| denotes absolute value

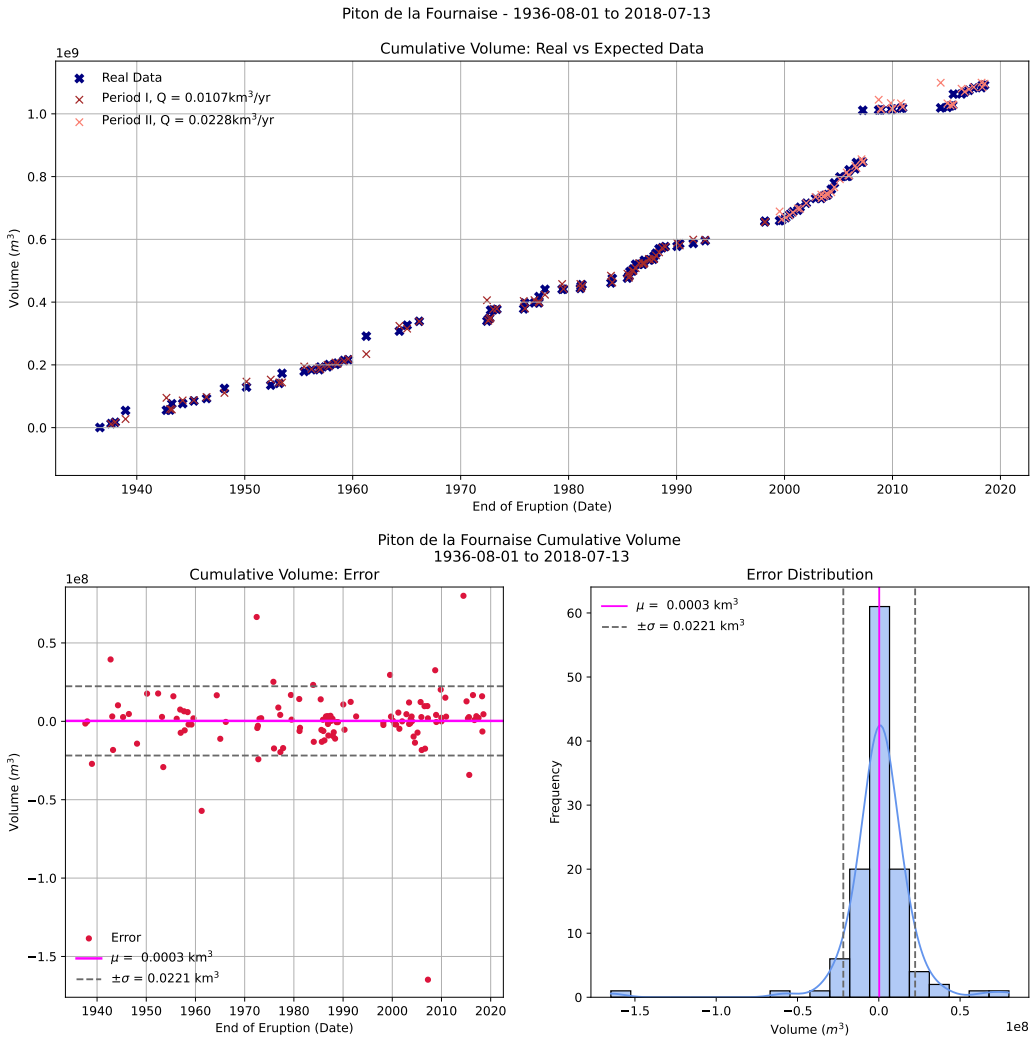

Figure 13: Piton, cumulative eruption volume: real data vs theorized from Eq. (1) with eruptive data from each period, and known time interval. TOP: Expected vs real data; BOTTOM LEFT: Error; BOTTOM RIGHT: Error distribution.

5 Additional Plots and Data

5.1 Linear Regression

Given a set of data points – specifically, the cumulative volume after each eruption over a period of interest – linear regression can be employed to fit the best line in the least-squares sense; that is, the line that minimizes the sum of squared differences between the observed data points and the corresponding points on the line.

Figure Fig.**(17)** (top) illustrates the linear regression applied to the cumulative volume across both periods studied. The corresponding error distribution is shown in Figure Fig.**(17)** (bottom), with error mean and standard deviation 0.0007 ± 0.0667 km^3; MAX error 0.1634 km^3 and RMSE 0.066747 km^3.

For the **linear regression** method (Sec. 3.2), we can force the line to pass through a specific datapoint (for example, the first cumulative volume of the period). The error is of similar behavior, but tends slightly to negative (underestimates the volume). Figure Fig.**(18)** (top) illustrates the linear regression applied to the cumulative volume across both periods studied, when we set the line to pass through the first datapoint. The corresponding error distribution is shown in Figure Fig.**(18)** (bottom), with an error of $0.0889 \pm 0.0667 km^3$, MAX of $0.1759 km^3$ and RMSE of 0.111129 km^3.

References

[1] O'Hagan, A., and Leonard, T. Bayes estimation subject to uncertainty about parameter constraints. *Biometrika 63*, 1 (1976), 201–203.

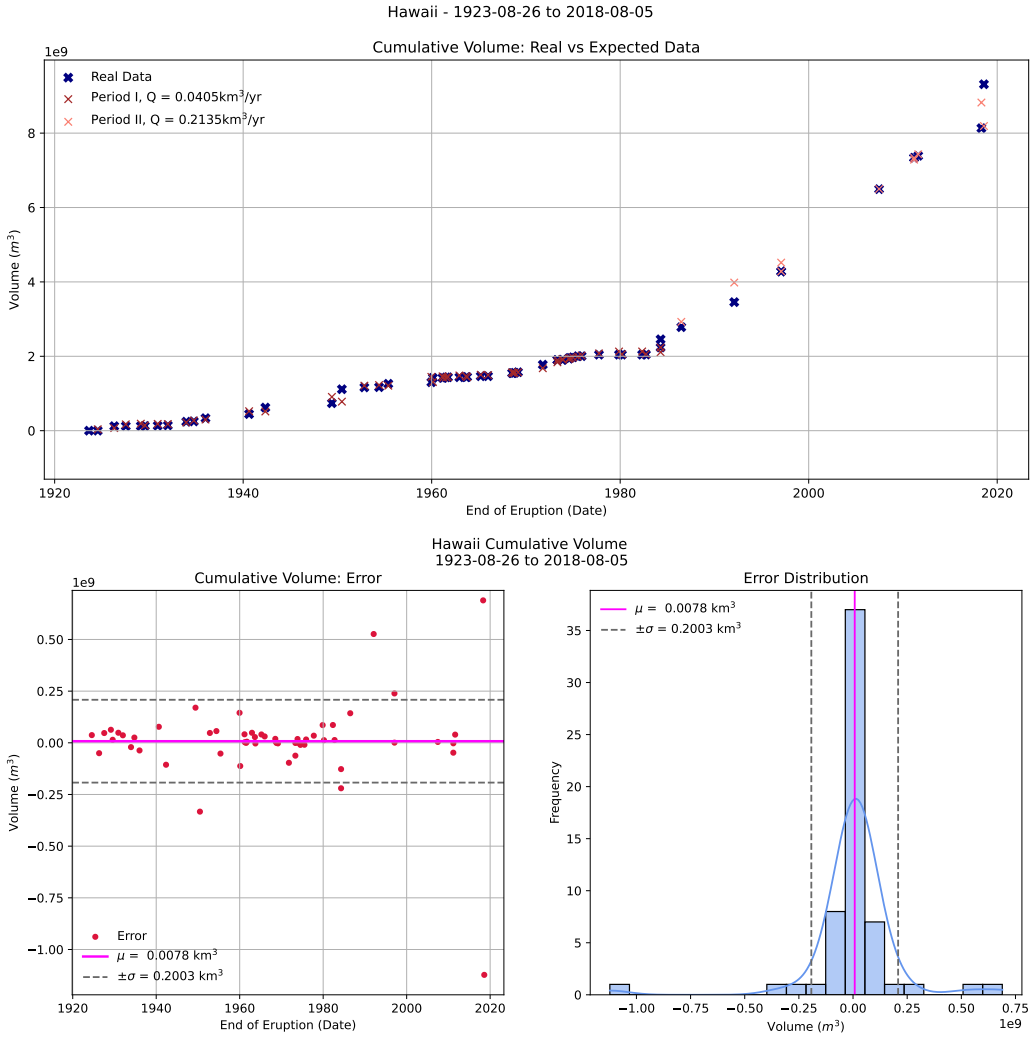

Figure 14: Hawaii, cumulative eruption volume: real data vs theorized from Eq. (1) with eruptive data from each period, and known time interval. TOP: Expected vs real data; BOTTOM LEFT: Error; BOTTOM RIGHT: Error distribution.

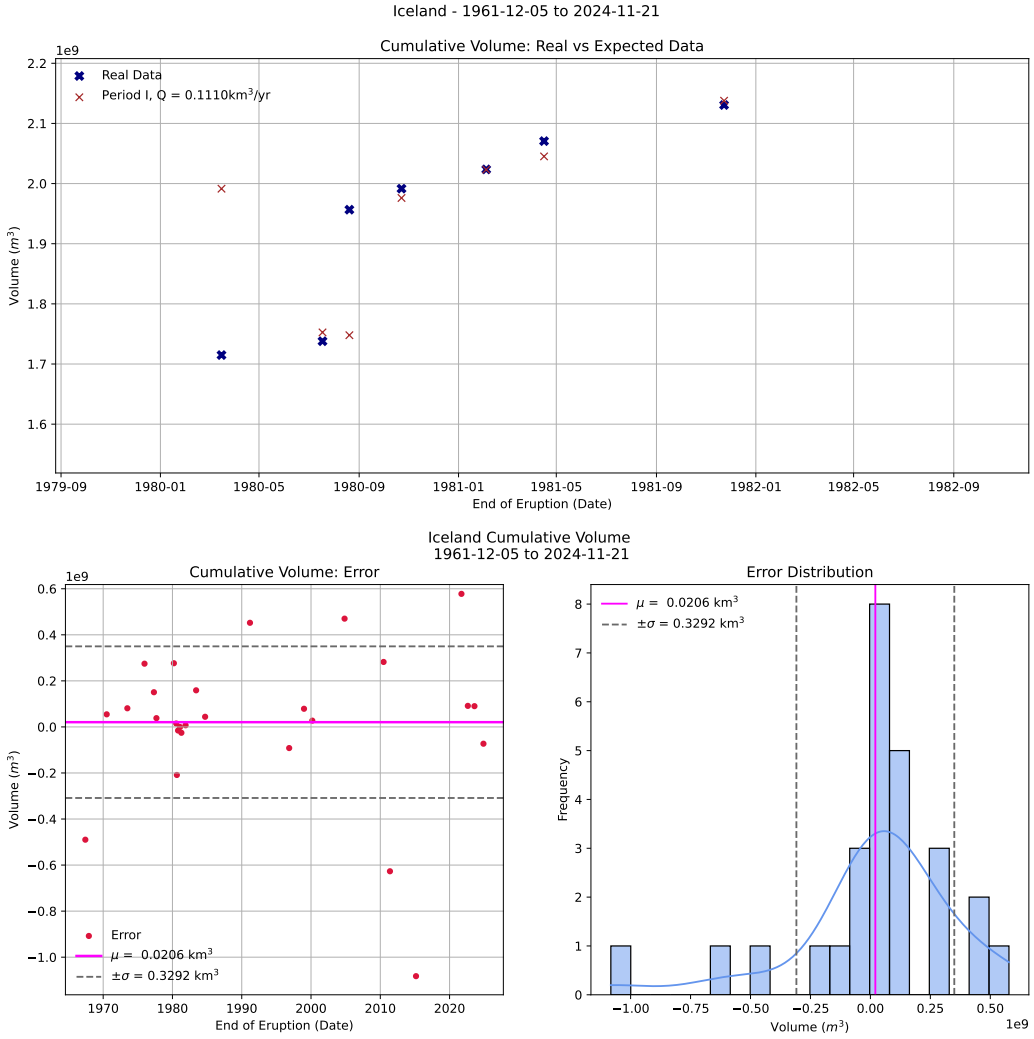

Figure 15: Iceland, cumulative eruption volume: real data vs theorized from Eq. (1) with eruptive data from each period, and known time interval. TOP: Expected vs real data; BOTTOM LEFT: Error; BOTTOM RIGHT: Error distribution.

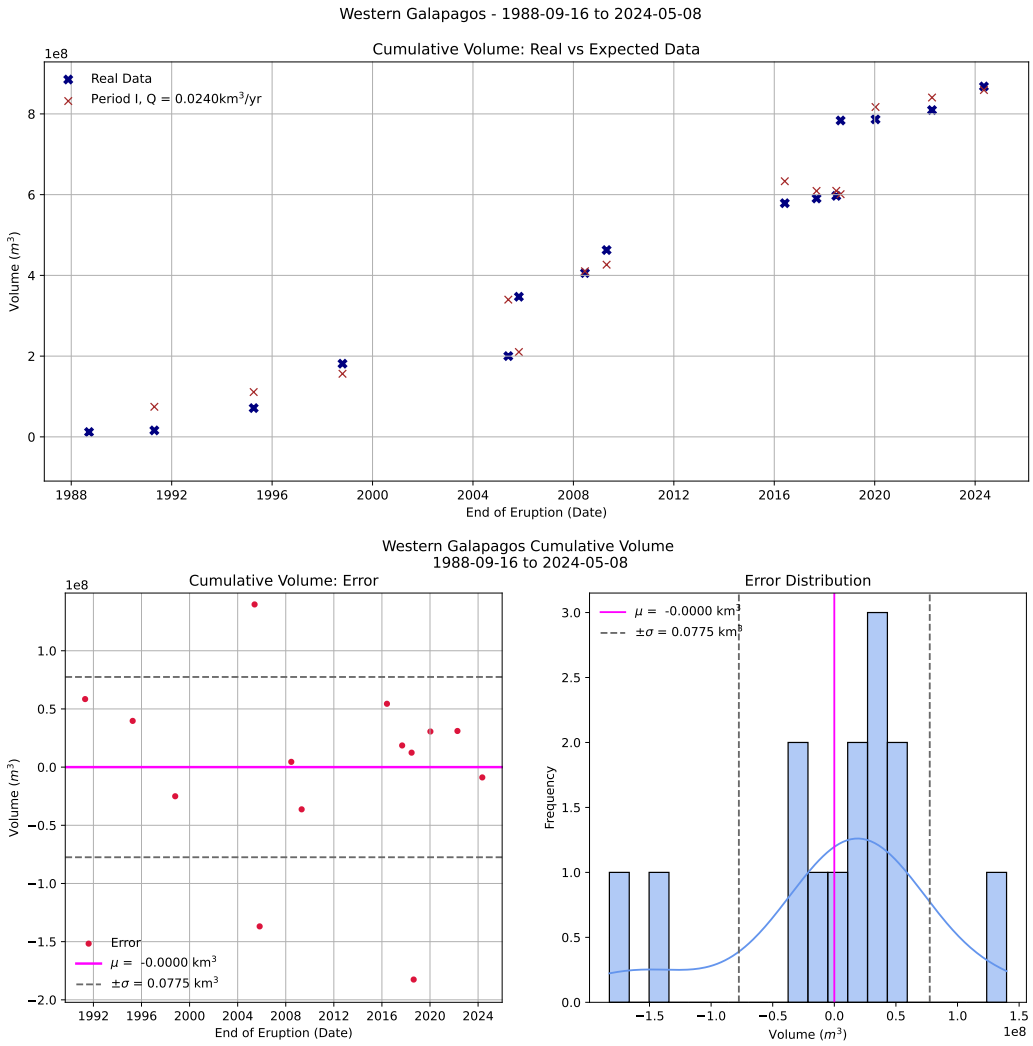

Figure 16: Galapagos, cumulative eruption volume: real data vs theorized from Eq. (1) with eruptive data from each period, and known time interval. TOP: Expected vs real data; BOTTOM LEFT: Error; BOTTOM RIGHT: Error distribution.

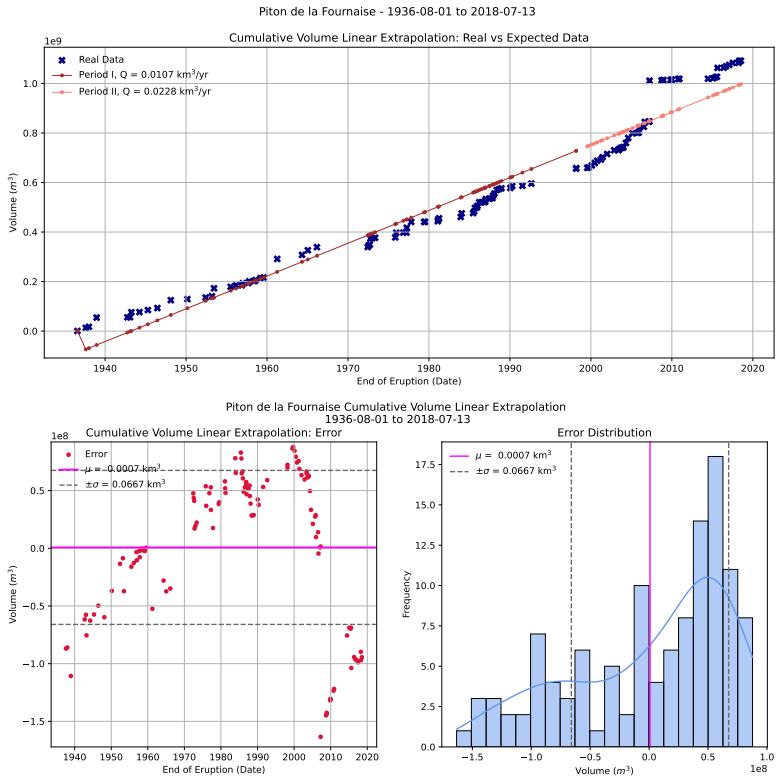

Figure 17: Cumulative eruption volume: real data vs linear regression (least squares). TOP: Expected vs real data; BOTTOM LEFT: Error; BOTTOM RIGHT: Error distribution.

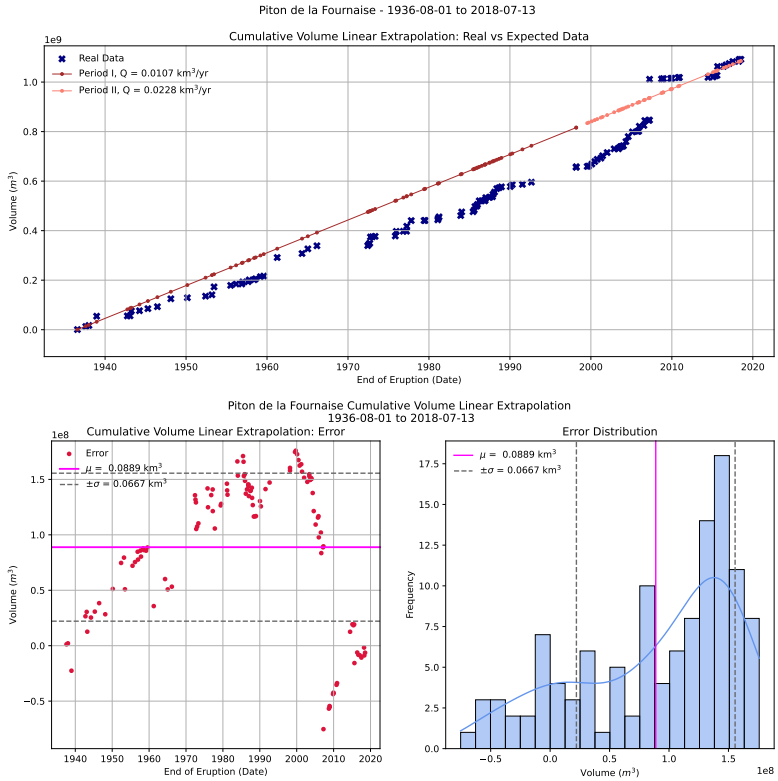

Figure 18: Cumulative eruption volume: real data vs linear regression with fixed initial volume. TOP: Expected vs real data; BOTTOM LEFT: Error; BOTTOM RIGHT: Error distribution.